

Article

A Distributed Control Strategy for Frequency Regulation in Smart Grids Based on the Consensus Protocol

Rong Fu *, Yingjun Wu, Hailong Wang and Jun Xie

College of Automation, Nanjing University of Posts and Telecommunications, Nanjing 210023, China; E-Mails: ywu_njupt@163.com (Y.W.); hailongwang1988@126.com (H.W.); jxie@njupt.edu.cn (J.X.)

* Author to whom correspondence should be addressed; E-Mail: furong@njupt.edu.cn; Tel.: +86-25-85-866-500.

Academic Editor: William Holderbaum

Received: 29 April 2015 / Accepted: 23 July 2015 / Published: 31 July 2015

Abstract: This paper considers the problem of distributed frequency regulation based on the consensus control protocol in smart grids. In this problem, each system component is coordinated to collectively provide active power for the provision of ancillary frequency regulation service. Firstly, an approximate model is proposed for the frequency dynamic process. A distributed control algorithm is investigated, while each agent exchanges information with neighboring agents and performs behaviors based on communication interactions. The objective of each agent is to converge to a common state considering different dynamic load characteristics, and distributed frequency control strategy is developed to enable the agents to provide active power support. Then, the distributed proportional integral controllers with the state feedback are designed considering the consensus protocol with topology \mathcal{G} . The theory of distributed consensus protocol is further developed to prove the stability of the proposed control algorithm. When properly controlled, the controllers can provide grid support services in a distributed manner that turn out the grid balanced globally. Finally, simulations of the proposed distributed control algorithm are tested to validate the availability of the proposed approach and the performance in the electrical networks.

Keywords: distributed control; consensus protocol; multi-agent system; dynamic loads; frequency regulation

1. Introduction

Inspired by the Smart Grid, electrical power systems are undergoing a global transformation in structure and functionality to increase efficiency and reliability. Such transformations are expanded by the introduction of new technologies such as advanced communication and control, integration of new flexible loads and new electricity generation sources. In smart electrical power networks, proper coordination and control of generation and load resources provide flexible frequency regulation services to enhance efficiency and reliability in smart grids. The distributed control strategies for coordination of distributed energy and load resources are proposed to provide active power for the provision of ancillary frequency regulations.

Traditionally, centralized frequency control is implemented and operated at different timescales in dispatching centering [1]. Automatic generation control (AGC) and governor control are adjusted to maintain the system frequency tightly around the nominal value when these distributed energy and load resources fluctuate uncertainly. The objective of the frequency controller is to keep the system frequency and the inter-area power transmission to the scheduled values during normal conditions, and when the system is subject to disturbances or sudden changes [2]. The primary frequency control operates at a timescale in minutes or so, and adjusts the operating points of governors in a centralized mode to drive the frequency back to its reasonable and secure value. Kothari *et al.* [3] have proposed an optimal PI controller by using area control error (ACE) stability control techniques. Malik *et al.* [4] have developed a generalized approach based on dual-mode discontinuous control and variable structure systems. Moon *et al.* [5] have devised a PID frequency controller to realize noise-tolerable differential control problems in power systems. Adaptive PI controllers are also proposed to regulate the power supply based on the self-tuning regulator. Yamashita *et al.* [6] have devised a method of designing a multi-variable self tuning-regulator for frequency problem on load demand. Khodabakhshian *et al.* [7] have proposed a new designed PID controller for automatic generation control in power systems.

Furthermore, decentralized control techniques have been used to deal with frequency control problems on the generation side. The robust decentralized controllers are designed independently, mainly based on the uses of a reduction model observer and a PI/PID controller. Yang *et al.* [8] have transformed the decentralized frequency controller design problem into an equivalent problem of controller design for a multi-port control system. Liu *et al.* [9] have proposed a new nonlinear constraint predictive control algorithm to guarantee the frequency dynamic stability. The design and operation of each local controller requires only its local states, and the errors between the outputs of two physical connected controllers are used to adaptively correct for the interactions from a global approximation model. Ilic *et al.* [10] have investigated a decentralized multi-agent frequency control system based on power communication technology. A robust load frequency controller is proposed to use genetic algorithms and linear matrix inequalities [11]. Nowadays, model free and data processing techniques also have been studied in control power generations to dump oscillations [12]. Some relative works are also proposed in literature [13] on the techniques of intelligent frequency control methods. It shows that decentralized control methods might provide efficient control with self-healing characters [14].

Recently, the distributed cooperative control manner for multi-agent systems has attracted increasing attention due to their flexibility and networked computational efficiency in many areas such as mobile robots, vehicle and traffic control. One kind of basic and challenging problem in distributed

cooperative control is the consensus problem for multi-agent systems. The coordination and synchronization process necessitates that each agent could exchange information with neighboring agents according to some restricted communication protocols and distributed algorithms [15,16]. Ilic *et al.* [17] have proposed a fully distributed frequency control algorithm for electrical power systems. A push-sum algorithm is used to adapt to the demand [18], and a modified consensus algorithm including weights in the network is proposed in distributed control [19]. Andreasson *et al.* [20] have studied the consensus algorithm for frequency control considering agents with system dynamics. Zhao *et al.* [21] have designed continuous distributed load control for primary frequency regulation and the Lyapunov function method is used to prove the convergence of the analytic model. It shows that distributed control methods might provide efficient control with self-healing characters. If all the agents on a network converge to a common state, we could make a decision that the consensus problem has been solved and the common state is called the consensus state of the agents.

In smart grids, new hierarchical model of frequency adjustment and the distributed control techniques are proposed considering distributed communication protocols [2]. The cooperative frequency control strategy is executed to achieve a primary and secondary frequency recovery using the optimized average consensus algorithm. Furthermore, utilizing load side control is an appealing alternative to control the system frequency on the demand side, which can reduce the dependency of grids on the expensive generation side controllers. Remarkably, it emphasizes that such frequency adaptive loads would allow the system to accept more readily a stochastically fluctuating energy source. It can be seen that the proposed distributed control has possible benefits over centralized frequency control [22].

Compared with the traditional centralized power regulation strategies, the distributed controllers have the following features: (i) The pressure of communication becomes more distributed between various distributed controller devices; (ii) The distributed resources can take decisions collectively from the network to achieve better quality and efficiency. While there are many studies and discussions in frequency control, there is not much analytic study that relates the behavior of the distributed frequency controllers with the dynamic behavior of the loads in smart grids.

In this paper, we further focus on the distributed primary frequency control on these energy resources and demand responses in smart grids. Considering the model of the power system dynamics by the swing equations, we apply and further develop the theory of distributed consensus to realize the stability of the proposed algorithm. The agents can reach an agreement on certain frequency deviations by sharing information locally with their neighbors. The analytic model and simulations exhibit that the proposed consensus protocol can attenuate the time-varying oscillations and lead the agents to steady state values for frequencies after disturbances.

The main structure and the content of this paper are organized as follows. In Section 2 (Consensus for Agents by Distributed Integral Action), we introduce the mathematical notation about the consensus protocol for the agents. In Section 3 (Network Model with Load Dynamics), we analyze the formulation of the frequency dynamic model and the consensus for agents. In Section 4 (Distributed Frequency Control Algorithm), based on the developed consensus protocol, we propose a distributed control algorithm for frequency control of electrical power systems, and compare the performance with traditional control algorithms. Simulation results of a two-area four-machine system using the proposed distributed control scheme are presented and discussed in Section 5 (Simulations). Finally, the conclusion of the distributed frequency control regulation is given in Section 6 (Conclusions).

2. Consensus for Agents by Distributed Integral Action

One basic and challenging problem in cooperative control is the consensus problem. It is assumed that there are multiple agents on a network. This network is usually modeled by a graph consisting of nodes (representing the agents) and edges (representing the interactions between agents). If all the agents on a network converge to a common state, we say that the multi-agent system solves a consensus problem or has a consensus property, and the common state is called group decision value or consensus state. This network is usually modeled by a graph consisting of nodes (representing the agents) and edges (representing the interactions between agents).

The proposed control architecture is illustrated including the distributed coordination frequency controller and the meshed electrical network describing the exchange of information among the multi-agents. For the application of frequency control in the electrical network, a connected and undirected graph \mathcal{G} of order n is considered with the set of nodes $\mathcal{V} = \{1, \dots, n\}$, set of edges $\mathcal{E} \subseteq \mathcal{V} \times \mathcal{V}$, and a weighted adjacency matrix $A = [a_{ij}]$ with nonnegative adjacency elements a_{ij} . In the undirected graph \mathcal{G} , the Laplacian matrix \mathcal{L} holds that $\mathcal{L} = \mathcal{B}(\mathcal{G})\mathcal{B}^T(\mathcal{G})$, where $\mathcal{B}(\mathcal{G})$ means the vertex-edge adjacency matrix of \mathcal{G} . I_n denotes the identity matrix of dimension n .

Consider the agents with second-order dynamics:

$$\begin{cases} \dot{r}_i = v_i \\ \dot{v}_i = u_i \\ u_i = - \sum_{j \in \mathcal{N}_i} (\beta(r_i - r_j) + \alpha(v_i - v_j)) + d_i \end{cases} \quad (1)$$

where $r_i \in \mathbb{R}^n$ and $v_i \in \mathbb{R}^n$ are the position and velocity states of the i th agent(node), u_i is the system input, $\alpha \in \mathbb{R}^+$ and $\beta \in \mathbb{R}^+$ are fixed parameters, and $d_i \in \mathbb{R}$ is a disturbance. \mathcal{N}_i denotes the set formed by all agent nodes connected to the node i .

Consider the linear coordinate change $z = \hat{S}^T v, w = \hat{S}^T r$, where $\hat{S} = \begin{bmatrix} \frac{1}{\sqrt{n}} & 1^{n \times 1} \\ S \end{bmatrix}$, S is a matrix such that \hat{S} is an orthonormal matrix. Thus the system dynamic (1) can be rewritten as:

$$\dot{z} = \begin{bmatrix} 0 & 0_{1 \times (n-1)} \\ 0_{(n-1) \times 1} & -\beta S^T L S \end{bmatrix} w + \begin{bmatrix} 0 & 0_{1 \times (n-1)} \\ 0_{(n-1) \times 1} & -\alpha S^T L S \end{bmatrix} z + \begin{bmatrix} \frac{1}{n} 1_{1 \times (n)} \\ S^T \end{bmatrix} d \quad (2)$$

We can eliminate the uncontrollable state w_1 and z_1 , thus obtaining the realization of the dynamic system by defining the new coordinates $w' = [w_2, \dots, w_n]^T$ and $z' = [z_2, \dots, z_n]^T$:

$$\begin{bmatrix} \dot{w}' \\ \dot{z}' \end{bmatrix} = \begin{bmatrix} 0_{(n-1) \times (n-1)} & I_{(n-1)} \\ -\beta S^T L S & -\alpha S^T L S \end{bmatrix} \begin{bmatrix} w' \\ z' \end{bmatrix} + \begin{bmatrix} 0_{(n-1) \times 1} \\ S^T d \end{bmatrix} \quad (3)$$

Since $S^T L S$ is invertible, the states w'' and z'' can be defined to consider the disturbance matrix transform.

$$\begin{bmatrix} w'' \\ z'' \end{bmatrix} = \begin{bmatrix} w' \\ z' \end{bmatrix} - \begin{bmatrix} 0_{(n-1) \times 1} \\ \frac{1}{\alpha} (S^T L S)^{-1} S^T d \end{bmatrix} \quad (4)$$

so in the new coordinates the system dynamics become:

$$\begin{bmatrix} \dot{w}'' \\ \dot{z}'' \end{bmatrix} = \underbrace{\begin{bmatrix} 0_{(n-1) \times (n-1)} & I_{(n-1)} \\ -\beta S^T L S & -\alpha S^T L S \end{bmatrix}}_{\triangleq A''} \begin{bmatrix} w'' \\ z'' \end{bmatrix} \tag{5}$$

The characteristic polynomial of A'' is given by $\det(\rho^2 I_{(n-1)} + (\alpha\rho + \beta)S^T L S)$. Compared with the characteristic polynomial $\det(sI + S^T L S)$, we note that the eigenvalues satisfy with solutions $-s_i < 0$ by lemma 10 in [23]. Since $S^T L S$ is full-rank, we obtain that the eigenvalues of A'' could satisfy $\det(\rho^2 + \alpha\rho s_i + \beta s_i) = 0$ with solutions $\rho \in \mathbb{C}^-$ by the Routh-Hurwitz stability criterion. Using the coordinates' shifts, it shows that the agents can converge to a common state and the consensus is reached for any $\alpha, \beta \in \mathbb{R}^+$.

3. Network Model with Load Dynamics

In the smart grid, the power system can be modeled by a graph $\mathcal{G} = (\mathcal{V}, \mathcal{E})$. There are two typical kinds of buses in the network: generator buses and load buses. The generator buses can convert the mechanical power into electric power and transmit them along the network. Then, the frequency dynamics on an i th synchronous generator can be modeled as follows:

$$\begin{cases} \dot{\delta}_i = \omega_i - \omega_{ref} \\ T_i \dot{\omega}_i = P_{mi} - P_{ei} - P_{di} - D_i \omega_i + u_i \end{cases} \quad \forall i \in \mathcal{V} \tag{6}$$

where δ_i is the phase angle of bus i , ω_i is the angular velocity of bus i , T_i and D_i are the inertia and damping coefficient, P_{mi} is the power injection at bus i , P_{ei} is the outputactive power of the generator i , P_{di} is the load at bus i , u_i is the mechanical input from frequency controller i . Let $P_{mi}^0, P_{ei}^0, P_{di}^0$ denote the initial uncontrolled operating point where $P_{mi}^0 - P_{ei}^0 - P_{di}^0 - D_i \omega_i^0 = 0$.

In general, load dynamics may diverge with the bus voltage magnitude (which is assumed fixed) and frequency. We distinguish between three types of loads, static controllable loads, frequency sensitive dynamic loads and uncontrollable loads. We assume that the frequency sensitive dynamic loads may increase linearly with frequency oscillations, and model these loads by $P_{di}(t) = P_{di}^0 + \Delta P_{di}(t) = P_{di}^0 + K_{di} \Delta \omega_i$, where K_{di} represents the load consumption due to the frequency deviation. Considering $P_{mi}(t) = P_{mi}^0 + \Delta P_{mi}(t)$, $P_{ei}(t) = P_{ei}^0 + \Delta P_{ei}(t)$, the deviation $\Delta P_{ei}(t)$ from the adjacent branch flows follows the linearized dynamic $\Delta P_{ei}(t) = \sum_{j \in \mathcal{N}_i} B_{ij} \cos(\Delta \delta_i^0 - \Delta \delta_j^0) (\Delta \delta_i - \Delta \delta_j)$, where $B_{ij} = \frac{|V_i||V_j|}{x_{ij}}$ is a constant determined by the operating bus voltages and the line reactance. We assume that the frequency deviations are small for all the buses $i \in \mathcal{V}$ and the differences between phase angle deviations are small across all the links in \mathcal{E} . Then, the deviation satisfy:

$$\begin{cases} \Delta \dot{\delta}_i = \Delta \omega_i \\ T_i \Delta \dot{\omega}_i = \Delta P_{mi} - \sum_{j \in \mathcal{N}_i} B_{ij} \cos(\Delta \delta_i^0 - \Delta \delta_j^0) (\Delta \delta_i - \Delta \delta_j) - K_{di} \Delta \omega_i - D_i \Delta \omega_i + u_i \end{cases} \quad \forall i \in \mathcal{V} \tag{7}$$

Let us consider the power system model by a graph $\mathcal{G} = (\mathcal{V}, \mathcal{E})$. Each energy resource node here is denoted by each agent, which is assumed to obey the linearized swing equation. The phased angle and the angular velocity of the agent i is δ_i and ω_i . By defining the state vectors $\delta = [\delta_1, \dots, \delta_n]$ and $\omega = \dot{\delta} = [\omega_1, \dots, \omega_n]$, we may rewrite (7) in state-space form as

$$\begin{bmatrix} \Delta \dot{\delta} \\ \Delta \dot{\omega} \end{bmatrix} = \begin{bmatrix} 0_{n \times n} & I_n \\ -M\mathcal{L}_k & -MK_d - MD \end{bmatrix} \begin{bmatrix} \Delta \delta \\ \Delta \omega \end{bmatrix} + \begin{bmatrix} 0_{n \times 1} \\ M\Delta P_m \end{bmatrix} + \begin{bmatrix} 0_{n \times 1} \\ Mu \end{bmatrix} \tag{8}$$

where $M = \text{diag}(\frac{1}{T_1}, \dots, \frac{1}{T_n}) = \text{diag}(M_1, \dots, M_n)$, $K_d = \text{diag}(K_{d1}, \dots, K_{dn})$, $D = \text{diag}(D_1, \dots, D_n)$, \mathcal{L}_k is the weighted Laplacian with agents edge weights k_{ij} , $k_{ij} = B_{ij} \cos(\Delta \delta_i^0 - \Delta \delta_j^0)$, $\Delta P_m = [\Delta P_{m1}, \dots, \Delta P_{mn}]^T$, $u = [u_1, \dots, u_n]^T$. The model (8) illustrates the power system dynamic behaviors. The system operates in an equilibrium point state where all frequency deviations are constant over time.

4. Distributed Frequency Control Algorithm

In this section, we design a distributed frequency controller based on the second-order consensus algorithm, where each agent measures its neighbors state information and integrates the relative differences. Compared with the traditional central controller, the distributed frequency controller solves the frequency control problem by several agents cooperatively, which results in better performance when an islanding network occurs or central signals are unavailable.

To control the agents reaching the consensus states, the controller of agent i from its adjacent agent j is assumed to be given by:

$$u_{ij} = -\alpha(\Delta \omega_i - \Delta \omega_j) - \beta(\Delta \delta_i - \Delta \delta_j) \tag{9}$$

We obtain a state feedback u_i which is designed based on a distributed protocol with topology \mathcal{G} . The distributed frequency controller can be designed as follows:

$$u_i = - \sum_{j \in \mathcal{N}_i} (\alpha(\Delta \omega_i - \Delta \omega_j) + \beta(\Delta \delta_i - \Delta \delta_j)) \quad \forall i \in \mathcal{V} \tag{10}$$

The protocol asymptotically solves the consensus problem when there exists an asymptotically stable equilibrium for all agent nodes. Then Equation (8) under the distributed Equation (10) can be given as:

$$\begin{bmatrix} \Delta \dot{\delta} \\ \Delta \dot{\omega} \end{bmatrix} = \underbrace{\begin{bmatrix} 0_{n \times n} & I_n \\ -M\mathcal{L}_k - M\beta I_n \mathcal{L}_k & -MK_d - MD - M\alpha I_n \mathcal{L}_k \end{bmatrix}}_{\triangleq A} \begin{bmatrix} \Delta \delta \\ \Delta \omega \end{bmatrix} + \begin{bmatrix} 0_{n \times 1} \\ M\Delta P_m \end{bmatrix} \tag{11}$$

It is easy to see that the characteristic equation of A can be given by $0 = \det((s^2 + MK_d s + MDs)I_n + (\alpha M + M + \beta M)\mathcal{L}_k)$. Let $\bar{m} = \min_i M_i$, $\bar{k} = \min_i K_{di}$ and $\bar{d} = \min_i D_i$. We may rewrite: $MK_d = \bar{m}\bar{k}I_n + K'$, and $MD = \bar{m}\bar{d}I_n + D'$, where K', D' are diagonal matrix with positive entries respectively. We now define the matrix $A' \triangleq \begin{bmatrix} 0_{n \times n} & I_n \\ -\bar{m}\mathcal{L}_k - \bar{m}\beta I_n \mathcal{L}_k & -\bar{m}\bar{k}I_n - \bar{m}\bar{d}I_n - \bar{m}\alpha I_n \mathcal{L}_k \end{bmatrix}$. The eigenvalues of A' are given by $\det((s^2 + s\bar{m}\bar{k} + s\bar{m}\bar{d})I_n + (s\bar{m}\alpha + \bar{m} + \bar{m}\beta)\mathcal{L}_k)$. By noticing that the characteristic equation of \mathcal{L}_k : $0 = \det(\mathcal{L}_k - \lambda_i I_n)$, where $\lambda_i \geq 0$, we can obtain the equations $s^2 + (s\bar{m}\alpha + \bar{m} + \bar{m}\beta)\lambda_i + s\bar{m}(\bar{k} + \bar{d}) = 0$. It shows that s must satisfy this equation for each λ_i . Considering $\alpha > 0, \beta > 0$, the above equation has all its solutions $s < 0$. In the translated coordinates, it follows that the matrix A is also Hurwitz. By simple calculation under the Routh-Hurwitz stability criterion, it can be seen that the aforementioned equation has its solutions $s \in \mathbb{C}^-$ if $\alpha, \beta \in \mathbb{R}^+$.

Given an initial position $\omega(0) = \omega_0$ under the dynamics (11), the power system is proved to be stable, hence, the consensus of the frequency $\lim_{t \rightarrow \infty} |\omega_i(t) - \omega_j(t)| = 0, \forall i, j \in \mathcal{V}$ is obtained.

With the adjustment of the controllable loads, their frequency regulation functions are distributed to each node agent. For the case in which $(\mathcal{V}, \mathcal{E})$ is a undirected and connected network, it guarantees that every trajectory converges to a compact set as $t \rightarrow \infty$ and $\omega(t)$ converges to an optimal point ω^* for the distributed frequency control.

So, several important features are illustrated:

- 1) Distributed Control. Each agent can make local decisions according to the local frequency and distributed coordination of power deviations. It allows a completely distributed solution and decreases the communication messages among the agents. A distributed control turns out to be gradually optimal with the coordination control of agents.
- 2) Equilibrium Frequency Objective. The frequency deviations $\omega(t)$ of agents are synchronized to ω^* no matter the transient dynamic difference. The new common frequency may be different from the initial frequency point when different disturbances occur. Mechanical power supplies and frequency-sensitive dynamic load consumptions are illustrated to drive the new system frequency regulation. Thus, an equilibrium frequency objective is proposed to converge to an optimal value.
- 3) Solution Optimization. The consensus algorithm by distributed integral dynamic action is developed to prove the stability of the frequency control problem. In an undirected and connected network, the consensus of the agents can be realized with distributed proportional-integral controllers. It illustrates that the trajectory of each agent can converge to the optimal frequency point ω^* to rebalance power flows after a disturbance.

5. Simulations

As a test system, a two-area four-machine system is provided to test the distributed frequency control algorithm [1]. The single line diagram of this system is given in Figure 1a. It consists of two areas and each area has two equivalent generators. The topology of communication network describing the exchange of information between generator agents is given in Figure 1b, where agents $A1$, $A2$, $A3$ and $A4$ represent generators G_1 , G_2 , G_3 and G_4 . In this network, there are three pairs of agents, namely $A1$ and $A2$, $A2$ and $A4$, $A4$ and $A3$, and the agents in each pair share information with each other.

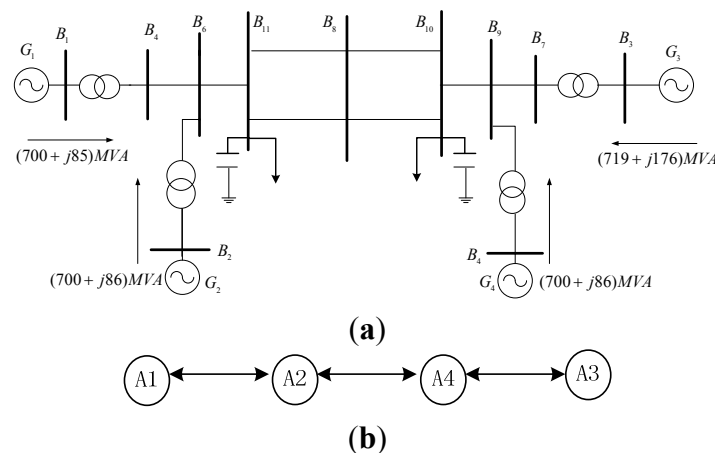


Figure 1. Two-area four-machine system. (a) Single line diagram; (b) The topology of communication network.

In our proposed method, generators are coordinated to collectively provide active power for the provision of ancillary frequency regulation service. We select loads in Bus 11 as controllable dynamic loads to perform load characteristic. The proportion of regulating frequency is -3% – 3% of the average loads in Bus 11. So $K_d = 0.2$ is defined to these controllable loads. These loads are controlled in frequency ancillary regulation and power damping.

In the simulation, we use the Power System Toolbox in MATLAB/SIMULINK to test closed-loop responses of controlled nonlinear systems. The simulation step size is 0.001 s. Unlike the proposed analytic model, the simulation model is much more detailed and realistic, including two-axis transient generator model, AC nonlinear power flows, and non-zero line resistances. The simulation would show whether our analytic model and control algorithm is a suitable approximation of the simulation model.

Considering multi-agent system with dynamics (8) and the communication topology given in Figure 1b, the Laplacian matrix is shown as $\mathcal{L}_k = \begin{bmatrix} -0.3557 & 0.3557 & 0 & 0 \\ 0.3557 & -0.4228 & 0 & 0.0671 \\ 0 & 0 & -0.3744 & 0.3744 \\ 0 & 0.0706 & 0.3744 & -0.4450 \end{bmatrix}$.

The simulations are conducted for different cases including the small signal disturbances and the short circuit faults. In addition, the system with various parameters for each of the cases are simulated. These simulations aim to check the robustness of distributed controllers obtained with parameter variations. Meanwhile, simulations for the system with different operating conditions are implemented for illustrating the effectiveness of the controller. For all simulations, detailed dynamic responses are considered. For evaluating the performance of the proposed controller, the integral of absolute frequency deviation, $J = \frac{1}{N} \sum_{i=1}^N \int_0^{\tau} \Delta f_i^2(t) dt$, is selected as a performance index. N is the total bus node number. The total time interval of τ for all simulations are taken as 20 s.

5.1. A Small Signal Disturbance and Stability Analysis

In this case, a small disturbance has occurred in the load demand. The system operates stability before the time of $t = 0$ s. At $t = 0$ s, there is a 1% step increase of the total demand. The frequency curve of the system for the case of without control is given in Figure 2. It shows that after the instant of load increase, the frequency of the system oscillates and the amplitude increases. Therefore, the system is prone to lose stability when small disturbance happens. In order to guarantee the system's stability, proper control schemes are required.

The proposed distributed frequency controllers are tested in the system operation. The power transmitted from area1 to area 2 through the tie-line for the cases of with and without the distributed frequency controller (DFC) are given in Figure 3. Without the DFC, the power oscillates and the amplitude increases largely. If frequency-sensitive load shedding control strategy is used in Bus 11, the curtailment of the loads is varied according to the frequency drop, which is fluctuated nearly from 16 MW to 10 MW around. The curve shows that the trajectories of the tie-line power continue oscillating at a long time. With the distributed frequency control and no dynamic loads, the power deviations converge to zero in less than 3 s. Considering DFC and dynamic load characteristics, the power oscillations could be damped faster. It can be seen that the performance of DFCs is more beneficial than load shedding control strategy. It also shows that considering dynamic loads' characters

for frequency regulations, the power transportation and frequency values can increase more than distributed frequency regulations without dynamic loads.

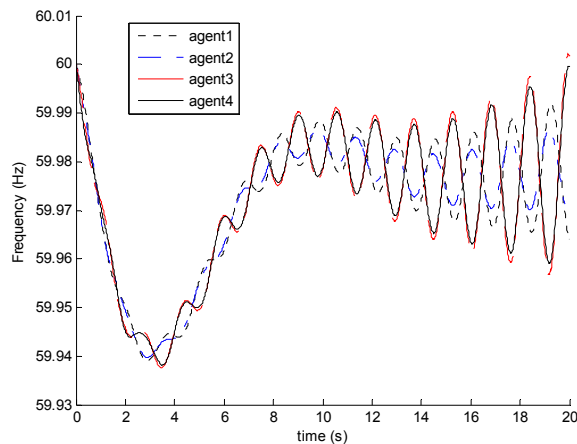


Figure 2. The frequency deviations without control in a small disturbance.

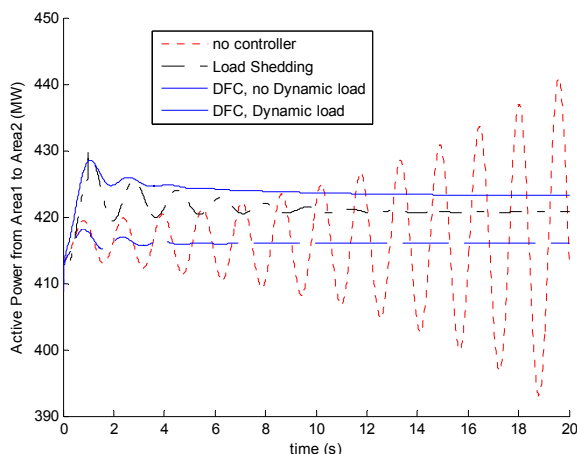


Figure 3. The tie-line active power (MW) *versus* time (s) with a small disturbance for cases (i) no controller; (ii) load shedding control; (iii) DFC without dynamic loads; (iv) DFC considering dynamic loads.

5.2. The Effects of Control Parameters of DFC on Frequency Stability

Previous simulation results indicate that the proposed method is capable to reduce the oscillation. In this section, we will discuss the effects of the control parameters, α and β , on power system frequency stability.

We first set β as zero to observe the effects of parameters α with various values. In fact, $\beta = 0$ means that the DFC cannot regulate the agents' angular acceleration. Figure 4a gives the frequency curves of system with different controller parameter α . From the figure, we found that the increase of parameter α brings a positive effect on damping frequency oscillations. Obviously, the control with the ability to regulate agents' angular acceleration would be more effective to damping frequency oscillations. Here we set $\alpha = 20$ to observe the effects of parameters β with various values. The simulation results are given in Figure 4b. It shows that the system frequency oscillation is suppressed. In addition, a smaller value of β indicates a better control performance.

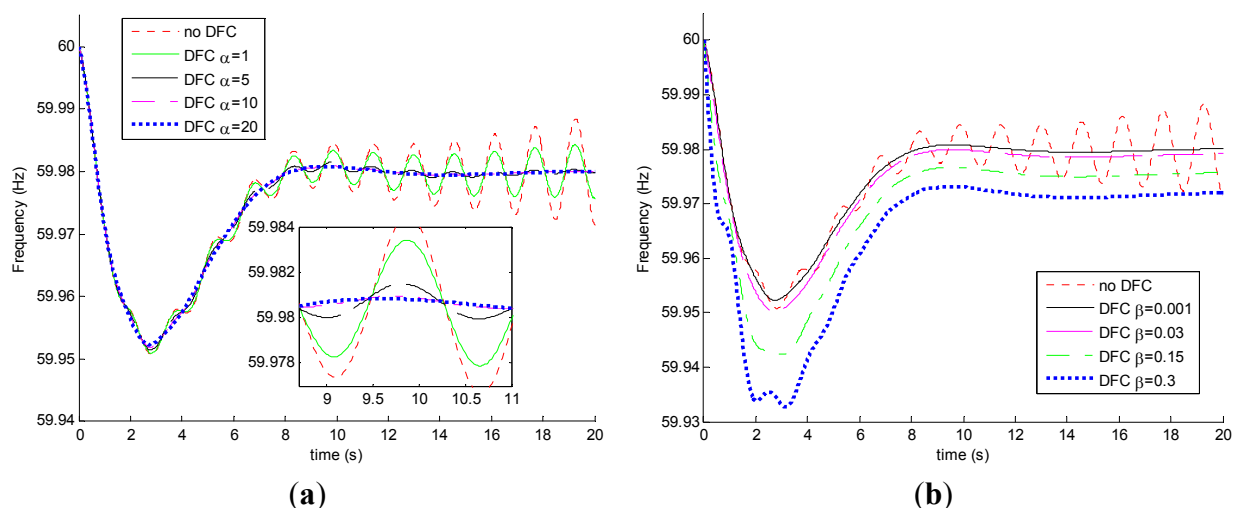


Figure 4. Comparisons of the frequency deviations under different controller parameters in a small disturbance (a) different α ($\beta = 0$); (b) different β ($\alpha = 20$).

The performance index of the system with different controller parameter α and $\beta = 0$ are calculated. The values of the performance index J and $\max\{\Delta f_1(t)\}$ are given in Table 1. In addition, the performance index of the system with different controller parameter β and $\alpha = 20$ are calculated. In Table 2, the values of J gradually increase with the increase of β . This is consistent with the observation that the larger β has a larger $\max\{\Delta f_1(t)\}$.

Table 1. The performance index under different controller parameters with the small disturbance ($\beta = 0$).

Different Controllers	J	$\max\{ \Delta f_1(t) \}$
NoDFC	0.0145	0.0492
DFC, $\alpha = 1$	0.0144	0.0491
DFC, $\alpha = 5$	0.0143	0.0485
DFC, $\alpha = 10$	0.0143	0.0481
DFC, $\alpha = 20$	0.0143	0.0477

Table 2. Different performances using different controller parameters with the small disturbance ($\alpha = 20$).

Different Controllers	J	$\max\{ \Delta f_1(t) \}$
NoDFC	0.0145	0.0492
DFC, $\beta = 0.001$	0.0144	0.0477
DFC, $\beta = 0.03$	0.0157	0.0497
DFC, $\beta = 0.15$	0.0215	0.0577
DFC, $\beta = 0.3$	0.0287	0.0673

It can be seen that frequency-sensitive loads have shown their frequency regulations in power networks. We also present simulation results below with different kinds of frequency-sensitive loads. Let K_d denote different kinds of frequency-sensitive loads, different consumption of the

frequency-sensitive loads are added on Bus 11. Thus, different kinds of frequency-sensitive load control performance are shown in Figure 5. In Figure 5a, the system has no controller, so that the different values of the parameter K_d cause different undamped oscillations. In Figure 5b, when the distributed frequency controllers are added, different values of the parameter K_d can contribute in the power balance and frequency regulation. It shows that these linear frequency-sensitive dynamic loads can rebalance power and resynchronize frequency after a disturbance. If K_d is larger, the load-side control time is often faster because of little time constants and evident load regulation solutions.

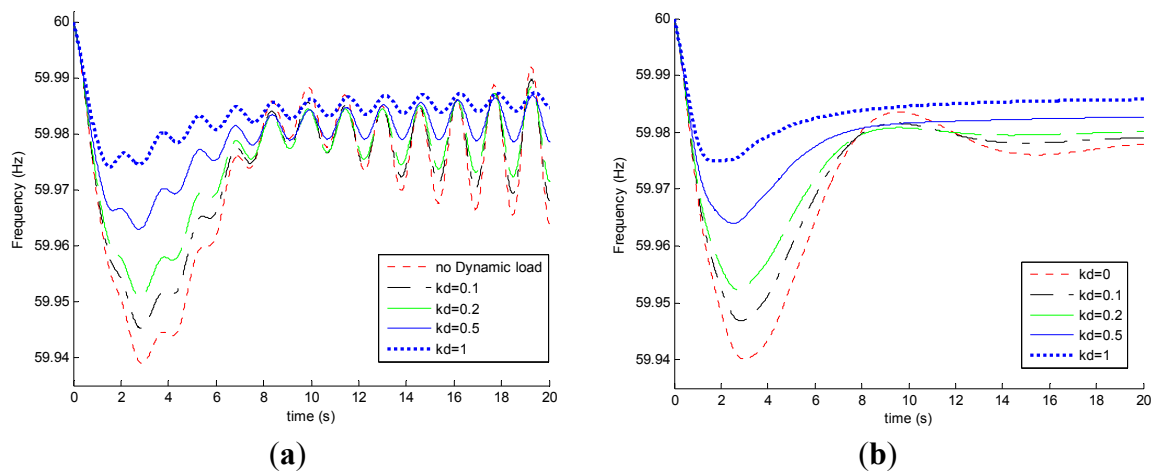


Figure 5. Comparisons of the frequency deviations under different dynamic load characteristics in a small disturbance. (a) No DFC; (b) with DFC.

5.3. A Short-Circuit Fault and Stability Analysis

In order to obtain more information to investigate the distributed controller performance in improving the system stability, transient stability simulations are tested to evaluate the results. A three-phase short-circuit fault is applied at bus8 at $t = 1$ s, which is cleared after $t = 200$ ms.

The power transmitted from area1 and area 2 after the fault is observed. As shown in Figure 6, with the distributed control, less fluctuation appears in the active power from area1 to area 2, and after a relatively short time (around 6 s) the power oscillation disappeared. It also shows that considering frequency-sensitive load regulation in a short circuit fault, the power transportation value could increase more than controllers without dynamic loads to improve system stability.

We also observed the frequency oscillation after the short circuit fault cleared. The curves of frequency oscillation of the system for the case with various α and $\beta = 0$ are given in Figure 7a. From the figure, it can be found that the system could keep stable when α is larger than 5. This means that the proposed DFC improves the transient stability if proper α is selected.

In Figure 7b, the curves of frequency oscillation after the short-circuit fault cleared for case with various β and $\alpha = 20$ are provided. Observing these curves, we saw that the systems keep stable for all combination patterns of α and β . For different combination patterns of α and β , the performance of the system are quitesimilar, which indicate that parameter β plays a less important role compared to parameter α . If α is larger, the damping control effect is more significant. In addition, a smaller value of β performs a better control effect in the long time.

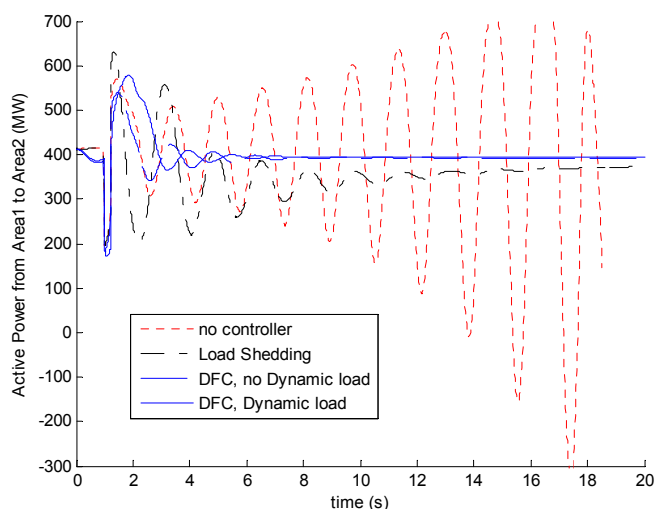


Figure 6. The tie-line active power (MW) from area1 to area2 when a three-phase short-circuit fault occurs (i) no DFC; (ii) load shedding control; (iii) DFC without dynamic loads; (iv) DFC considering dynamic loads.

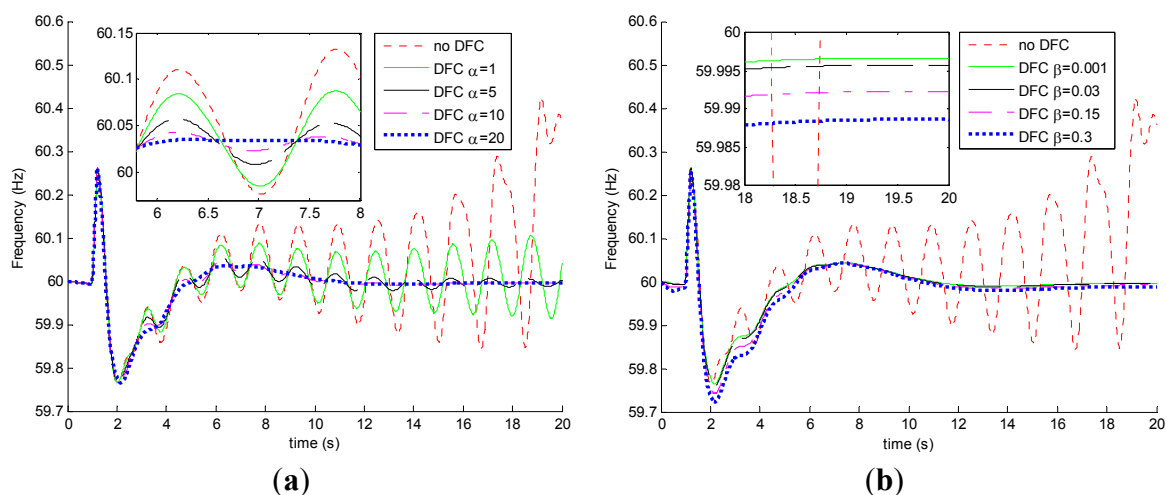


Figure 7. Comparisons of the frequency deviations under different controller parameters with a short-circuit fault (a) different α ; (b) different β ($\alpha = 20$).

Tables 3 and 4 provide the values of the performance indices for the cases of various combination patterns of parameters. These performance indices give the quantitative control evaluation values under different controller parameters.

Table 3. The performance index under different controller parameters with a short-circuit fault ($\beta = 0$).

Different Controllers	J	$\max \{ \Delta f_1(t) \}$
NoDFC	0.3875	0.4230
DFC, $\alpha = 1$	0.1132	0.2591
DFC, $\alpha = 5$	0.0771	0.2600
DFC, $\alpha = 10$	0.0765	0.2607
DFC, $\alpha = 20$	0.0799	0.2616

Table 4. The performance index using different controller parameters with a short-circuit fault disturbance ($\alpha = 20$).

Different Controllers	J	$\max \{ \Delta f_i(t) \}$
NoDFC	0.3875	0.4230
DFC, $\beta = 0.001$	0.0866	0.2645
DFC, $\beta = 0.03$	0.0829	0.2602
DFC, $\beta = 0.15$	0.0949	0.2558
DFC, $\beta = 0.3$	0.1096	0.2730

Figure 8a shows the phase plane diagram of frequency oscillation for the case without DFC. The agents' frequencies oscillate and finally the system turns into being in an unstable state. Then, we install DFC to each of these agents. The phase plane diagram of frequency oscillation is given in Figure 8b. In the figure, the state of each agent deviates from its original state, and after a certain time, goes back to the original state. This means that the DFC can keep the frequencies stable in the case of short-circuit fault occurred.

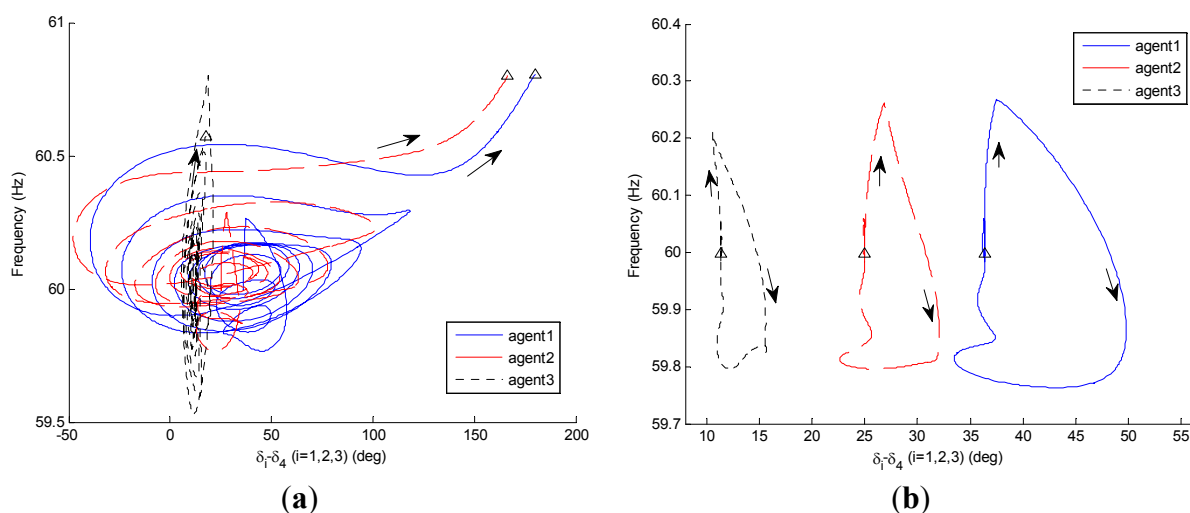


Figure 8. The phase plane diagram under (a) no DFC; (b) DFC with a short-circuit fault disturbance.

In summary, it can be concluded that the distributed frequency control can provide a guarantee of more reliable and stable power supply in the power system. The controller improves both the steady-state and transient performance of frequency. Compared with the central frequency control, the distributed frequency control method is more secure and efficient.

6. Conclusions

This paper develops a distributed control method to decide the active injection of the frequency regulation in the electrical network. Each distributed resource in the network computes the amount of active power that it needs to provide. A distributed frequency controller is designed considering the dynamic load characteristics, where each bus controls its own frequency based on local measurements and information from neighbouring places. For the purpose of designing the coordination controller,

some dynamic assumptions are made, *i.e.*, the difference between phase angles of buses are small, and the frequency sensitivities with respect to changes in the operating point do not change much for different operating points. The proposed consensus protocol can provide grid support services in a distributed manner and achieve the frequency regulation consensus. The simulations illustrate the availability to regulate frequency oscillations during the power dynamic process.

Acknowledgments

This work has been partially funded by the State Grid Corporation of China Project: Study on Key Technologies for Power and Frequency Control of System with ‘Source-Grid-Load’ Interactions, and the Six Talent Summit Project in Jiangsu Province.

Author Contributions

Rong Fu and Yingjun Wu contributed in developing the ideas of this research and the consensus algorithm in the paper. Rong Fu, Hailong Wang and Jun Xie performed this research and simulated the power system operations, all the authors involved in preparing this manuscript.

Conflicts of Interest

The authors declare no conflict of interest.

References

1. Kundur, P. *Power System Stability and Control*, 2nd ed.; McGraw Hill: New York, NY, USA, 2008.
2. Zhao, C.; Topcu, U.; Low, S.H. Optimal load control via frequency measurement and neighborhood area communication. *IEEE Trans. Power Syst.* **2013**, *28*, 3576–3587.
3. Kothari, M.L.; Nanda, J.; Kothari, D.P.; Das, D. Discrete-mode automatic generation control of a two-area reheat thermal system with new area control error. *IEEE Trans. Power Syst.* **1989**, *4*, 730–738.
4. Malik, O.P.; Kumar, A.; Hopeg, S. A load frequency control algorithm based on a generalized approach. *IEEE Trans. Power Syst.* **1988**, *3*, 375–382.
5. Moon, Y.H.; Ryu, H.S.; Lee, J.G.; Kim, S. Power system load frequency control using noise-tolerable PID feedback. In Proceedings of the IEEE International Symposium on Industrial Electronics, Pusan, Korea, 12–16 June 2001; Volume 3, pp. 1714–1718.
6. Yamashita, K.; Miyagi, H. Multi-variable self-tuning regulator for load frequency control system with interaction of voltage on load demand. *IEEE Proc. Control Theory Appl.* **1995**, *138*, 177–183.
7. Khodabakhshian, A.; Hooshmand, R. A new PID controller design for automatic generation control of hydro power systems. *Int. J. Electr. Power Energy Syst.* **2010**, *32*, 375–382.
8. Yang, T.C.; Cimen, H. Applying structured singular values and a new LQR design to robust decentralized power system load frequency control. In Proceedings of the IEEE International Conference on Industrial Technology, Shanghai, China, 2–6 December 1996; pp.880–884.
9. Liu, X.; Kong, X.; Deng, X. Power system model predictive load frequency control. In Proceedings of the American Control Conference, Montreal, QC, Canada, 27–29 June 2012; pp. 6602–6607.

10. Ilic, M.D.; Xie, L.; Khan, U.A.; Moura, J.M. Modeling of future cyber-physical energy systems for distributed sensing and control. *IEEE Trans. Syst. Man Cybern.* **2010**, *40*, 825–838.
11. Rerkpreedapong, D.; Hasanovic, A.; Feliachi, A. Robust load frequency control using genetic algorithms and linear matrix inequalities. *IEEE Trans. Power Syst.* **2003**, *18*, 855–861.
12. Yin, S.; Li, X.; Gao, H.; Kaynak, O. Data-based techniques focused on modern industry: An overview. *IEEE Trans. Ind. Electron.* **2014**, *62*, 657–667.
13. Kocaarslan, I.; Çam, E. Fuzzy logic controller in interconnected electrical power systems for load-frequency control. *Int. J. Electr. Power Energy Syst.* **2005**, *27*, 542–549.
14. Chidambaram, I.A.; Velusami, S. Design of decentralized biased controllers for load-frequency control of interconnected power systems. *Electr. Power Compon. Syst.* **2005**, *33*, 1313–1331.
15. Carli, R.; Chiuso, A.; Schenato, L.; Zampieri, S. Distributed Kalman filtering based on consensus strategies. *IEEE J. Sel. Areas Commun.* **2008**, *26*, 622–633.
16. Liu, W.; Gu, W.; Sheng, W.; Meng, X.; Wu, Z.; Chen, W. Decentralized multi-agent system-based cooperative frequency control for autonomous microgrids with communication constraints. *IEEE Trans. Sustain. Energy* **2014**, *5*, 446–456.
17. Ilic, M.D.; Liu, Q. Toward sensing, communications and control architectures for frequency regulation in systems with highly variable resources. In *Control and Optimization Methods for Electric Smart Grids*; Springer: New York, NY, USA, 2012; Volume 3, pp. 3–33.
18. Molina-Garcia, A.; Bouffard, F.; Kirschen, D.S. Decentralized demand-side contribution to primary frequency control. *IEEE Trans. Power Syst.* **2011**, *26*, 411–419.
19. Pedroche, F.; Rebollo, M.; Carrascosa, C.; Palomares, A. On the convergence of weighted-average consensus. *Int. J. Elec. Power Energy Syst.* **2013**, arXiv:1307.7562v1.
20. Andreasson, M.; Sandberg, H.; Dimarogonas, D.V.; Johansson, K.H. Distributed integral action: Stability analysis and frequency control of power systems. In Proceedings of the IEEE 51st Annual Conference on Decision and Control, Maui, HI, USA, 10–13 December 2012; pp. 2077–2083.
21. Zhao, C.; Topcu, U.; Li, N.; Low, S. Design and stability of load-side primary frequency control in power systems. *IEEE Trans. Autom. Control* **2014**, *59*, 1177–1189.
22. Yu, W.; Chen, G.; Cao, M. Some necessary and sufficient conditions for second-order consensus in multi-agent dynamical systems. *Automatica* **2010**, *46*, 1089–1095.
23. Freeman, R.A.; Yang, P.; Lynch, K.M. Stability and convergence properties of dynamic average consensus estimators. In Proceedings of the 45th IEEE Conference on Decision and Control, San Diego, CA, USA, 13–15 December 2006; pp. 2398–2403.